JACS
JOURNAL OF THE AMERICAN CHEMICAL SOCIETY

Article

pubs.acs.org/JACS

Bridging Adhesion of a Protein onto an Inorganic Surface Using Self-Assembled Dual-Functionalized Spheres

Sota Sato,*[,†] Masatoshi Ikemi,[†] Takashi Kikuchi,[†] Sachiko Matsumura,[‡] Kiyotaka Shiba,*[,‡] and Makoto Fujita*[,†]

[†]Department of Applied Chemistry, School of Engineering, The University of Tokyo, 7-3-1 Hongo, Bunkyo-ku, Tokyo 113-8656, Japan

[‡]Division of Protein Engineering, Cancer Institute, Japanese Foundation for Cancer Research, 3-8-31 Ariake, Koto-ku, Tokyo 135-8550, Japan

Supporting Information

ABSTRACT: For the bridging adhesion of different classes of materials in their intact functional states, the adhesion of biomolecules onto inorganic surfaces is a necessity. A new molecular design strategy for bridging adhesion was demonstrated by the introduction of two independent recognition groups on the periphery of spherical complexes self-assembled from metal ions (M) and bidentate ligands (L). These dual-functionalized $M_{12}L_{24}$ spheres were quantitatively synthesized in one step from two ligands, bearing either a biotin for streptavidin recognition or a titania-binding aptamer, and Pd(II) ions. The selective recognition of titania surfaces was achieved by ligands with hexapeptide aptamers (Arg−Lys−Leu−Pro−Asp−Ala: minTBP-1), whose fixation ability was enhanced by the accumulation effect on the surface of the $M_{12}L_{24}$ spheres. These well-defined spherical structures can be specifically tailored to promote interactions with both titania and streptavidin simultaneously without detrimentally affecting either recognition motif. The irreversible immobilization of the spheres onto titania was revealed quantitatively by quartz crystal microbalance measurements, and the adhesion of streptavidin to the titania surface mediated by the biotin surrounding the spheres was visually demonstrated by lithographic patterning experiments.

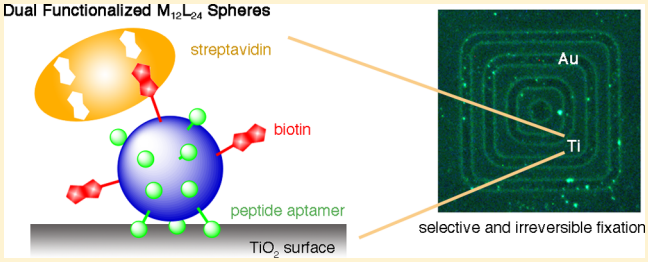

INTRODUCTION

Bridging adhesion of biomolecules onto inorganic surfaces without preprocessing is an important fundamental technique that has been developed for analytical methods in order to reveal biological functions. Anchoring biomolecules onto a sensor tip can convert the interaction with the corresponding substrate into an electric signal or fluorescent output, which allows for the interaction to be quantified. Some examples include an antibody-immobilized chip that has been applied for the diagnosis of diseases by the detection of an antigen-like virus,[1] DNA strands of different sequences that have been displayed on a chip in order to detect the complementary DNA,[2] and proteins that have been arrayed on a chip to identify the binding proteins or to construct continuous flow reactor systems.[3]

Beyond analytical applications, these unique materials, known as "biominerals" when produced in nature, that are composed of inorganic materials and biomolecules have attracted the attention of chemists[4] due to their strong yet light material properties, which many different creatures exploit in order to construct their exoskeletal supports. These exquisite mechanical properties are suitable for applications in regenerative medicine, and many efforts have been made to "glue" normally irreconcilable biomolecules with stable metals through surface modification of that metal.[5] Titanium is one of the most promising materials because of its excellent mechanical properties, including corrosion resistance, which make it suitable as an implant material in the treatment of certain oral conditions.[6] To overcome the weak cell-binding properties of titanium, protein modification on the surface of titanium (i.e., titania) has been examined, and the key to glue titanium to cells has been found to be a sequence-modified protein bearing both titania-binding and cell-binding peptides.[7] The peptide that recognizes inorganic surfaces is called a material-binding peptide aptamer, which noncovalently binds to a specific inorganic surface without premodification.[8] The peptide aptamer is easily synthesized and can be introduced into proteins during artificial synthesis or genetic modification. The binding affinity of each peptide aptamer is generally not strong, but the accumulative effect has been demonstrated to be enough in order to realize firm fixation.

We have developed the synthesis of designable spheres by self-assembly based on coordination chemistry[9] with component ligands that can be decorated with a variety of functional groups. When transition metal ions (M) and bidentate ligands

Received: June 14, 2015
Published: July 19, 2015

DOI: 10.1021/jacs.5b06184
J. Am. Chem. Soc. 2015, 137, 12890−12896

(L) are mixed in solution, a family of M_nL_{2n} spheres is efficiently synthesized.[10] The outside and/or inside of the sphere can be modified with functional groups that can be introduced to the starting ligand before the self-assembly of the sphere takes place. Once assembled, these functional groups densely accumulate, yielding a characteristic localized environment on the surface and/or in the cavity of the spheres. These localized environments can be exploited to selectively recognize small organic molecules[11] or large biomolecules[12] and to effectively work as templates for inorganic nanomaterial syntheses.[13] In spite of these cumulative examples, spheres bearing different functional groups for the simultaneous recognition of different targets have not been reported.

A titania-binding peptide aptamer, known as the minTBP-1 hexapeptide aptamer (Arg−Lys−Leu−Pro−Asp−Ala), has been developed by the phage display method,[14] and reversible binding on titania was observed when 20 of the peptide aptamers were introduced at the periphery of ferritin, a protein with a diameter of 12 nm (the surface density of the peptide aptamer was 0.044 chain/nm^2).[15] The binding affinity of the ferritin, which was decorated with the peptide aptamers on its surface, was enhanced by 2 orders of magnitude compared to that of a single peptide aptamer. In previous work, we showed that an $M_{12}L_{24}$ sphere with a diameter of 3.5 nm decorated with 24 minTBP-1 peptide aptamers showed even stronger irreversible binding on titania due to the increased surface density of the peptide aptamer (0.62 chain/nm^2).[16] This irreversible recognition was realized by the accumulation of electrostatic interactions between the conformationally rigid basic Arg and acidic Asp residues of the peptide aptamers and titania.

Here, we focus on the dual functionalization at the periphery of $M_{12}L_{24}$ spheres, which contain a mixture of two ligands that are functionalized with either the peptide aptamer for titania binding or a protein-binding site, which shows specific recognition for both the inorganic surface and the target protein. We envisioned that the surface density of peptide aptamers on the $M_{12}L_{24}$ sphere would still be sufficiently high to maintain the enhanced binding affinity on titania even when several of the peptide aptamer appended ligands are replaced with protein-binding residues. Biotin was selected as a model protein recognition site due to the well-established biotin−streptavidin motif.[17] We also envisioned that the high stability[18] of the self-assembled $M_{12}L_{24}$ spheres supported by 48 coordination bonds would be sufficient to maintain its structure even after adhesion of the protein aptamer onto the titania surface. We synthesized the dual-functionalized $M_{12}L_{24}$ spheres by the self-assembly of Pd(II) ions with a bent ligand bearing the minTBP-1 aptamer and another bent ligand bearing a biotin. These spheres show irreversible fixation onto titania, after which streptavidins could be selectively fixed onto the titania via the "gluing" interaction of biotin on the periphery of the spheres.

RESULTS AND DISCUSSION

We previously reported the synthesis of the $M_{12}L_{24}$ sphere **2a** from the ligand **1a**, bearing the minTBP-1 peptide aptamer, and palladium(II) ions and demonstrated that the sphere **2a** displaying 24 minTBP-1 peptide aptamers on its surface realizes selective fixation of the spheres onto titania (Figure 1).[16] The diameter of the $M_{12}L_{24}$ skeleton is 3.5 nm, and that of the whole molecule is 8.8 nm. The irreversible immobilization of the sphere on the titania surface was evidenced by atomic force microscopy data and quartz crystal microbalance (QCM) analysis.

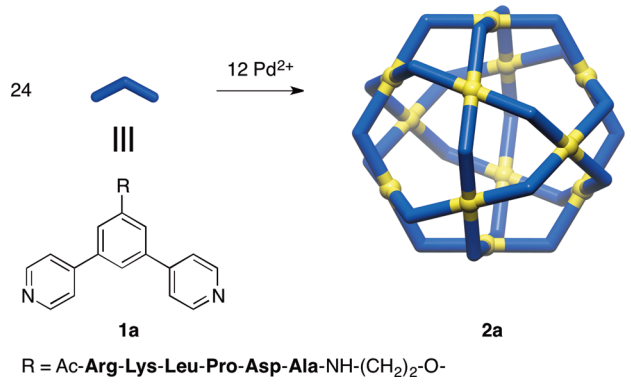

Figure 1. Self-assembly of sphere **2a** decorated with 24 minTBP-1 peptide aptamers from 24 ligands of **1a** bearing the peptide and 12 palladium(II) ions.

Here, we have added protein recognition through the replacement of several titania-binding peptide aptamers with biotin in order to realize the effective fixation of streptavidin onto the titania surface. We designed new ligands in which biotin was attached to the convex edge of the ligand by means of either a long peptide linker (**1b**) or a short linker (**1c**) (Figure 2a). Ligand **1b** was designed in such a way as to allow the biotin to extend beyond the reach of the peptide aptamer hexapeptide minTBP-1 once ligands **1a** and **1b** have been mixed and complexed with Pd(II) ions, forming the sphere, enabling exposure and therefore capture of at least one streptavidin on the densely modified surface. The ligand **1c** was designed for a control experiment, constructing a sphere using both ligands **1a** and **1c** in order to prove the exposure effect, wherein the biotin moieties should be buried within the minTBP-1 aptamers and sterically isolated from contact with streptavidin. The ligand **1b** was synthesized in 43% yield from three steps starting with the H-Ala-2-Cl-trt resin, amino acids, and biotin, eventually affording a protected peptide bearing a biotin by Fmoc solid-phase peptide synthesis. A subsequent tethering reaction to the ligand precursor **1e** using a HBTU−HOBt−DIPEA synthetic protocol followed by a cleavage reaction of the peptide protecting groups with trifluoroacetic acid (see Supporting Information) yielded the target ligand. The ligand **1c** was synthesized in 77% yield by the coupling of biotin and the ligand precursors **1e** using the HBTU−HOBt−DIPEA protocol. The ligand **1d** and the ligand precursor **1e** were synthesized using previously reported procedures.[16]

With the synthesized ligands in hand, we first examined the formation of the dual-functionalized spherical complex **3a** composed of the bent ligand bearing the minTBP-1 aptamer and the one bearing biotin in a 3:1 ratio. The quantitative formation of the $M_{12}L_{24}$ spherical complex **3a**, consisting of ligands **1a** and **1b** in 3:1 molar ratio, was observed when ligands **1a** (11.1 mg, 7.50 μmol) and **1b** (4.35 mg, 2.50 μmol) were treated with $Pd(NO_3)_2$ (1.61 mg, 7.00 μmol) in dimethylsulfoxide (DMSO, 1.0 mL) at 70 °C for 24 h. The single set of proton resonances in the ^{1}H NMR spectrum arising from the pyridyl groups indicates that the two ligands are uniformly distributed throughout the structure of the spherical complex (Figure 2b). The observation of broadened signals is typically exhibited by very large complexes that tumble slowly on the NMR time scale. The size of the product was estimated by the

DOI: 10.1021/jacs.5b06184
J. Am. Chem. Soc. 2015, 137, 12890−12896

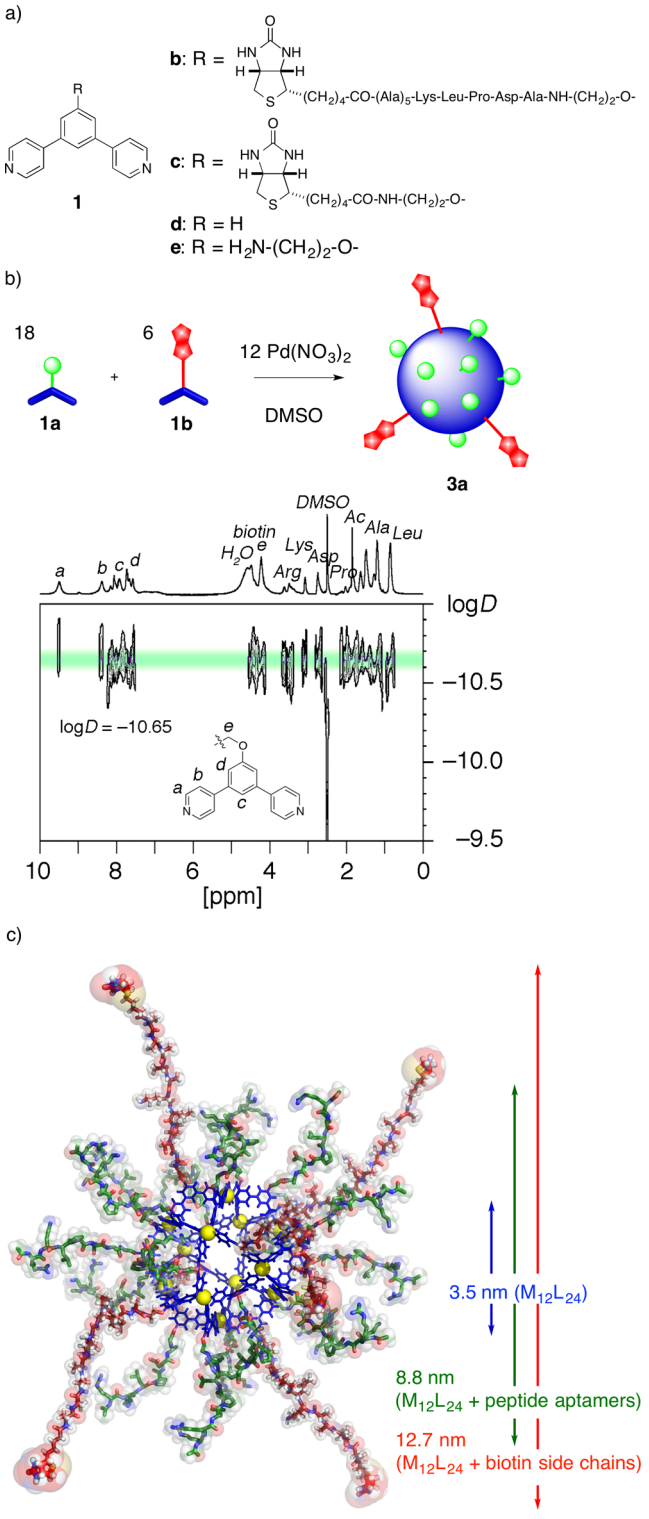

Figure 2. (a) Structures of the biotin-functionalized ligands with a long linker (**1b**), a short linker (**1c**), an unsubstituted ligand **1d**, and a ligand precursor **1e**. (b) Synthesis and ^{1}H DOSY NMR spectra of sphere **3a** (500 MHz, DMSO-d_6, 27 °C). (c) Optimized molecular structure of sphere **3a** (blue, the framework of the $M_{12}L_{24}$ sphere; yellow, Pd ions; mostly green chains, minTBP-1 peptide aptamers; and mostly red chains, the side chains tethering biotins at their terminals).

diffusion coefficient determined by diffusion-ordered NMR spectroscopy (DOSY). All the signals of the product sphere **3a** in DMSO showed the same diffusion coefficient, D = 2.2 × 10^{-11} m^2 s^{-1}, appearing as a single band in the 2D spectrum, an observation which further corroborates that the spheres are constructed from uniformly mixed ligands (Figure 2c). The D value is consistent with that of the sphere **2a** self-assembled from ligand **1a** and Pd(II) ions using an identical protocol (D = 3.8 × 10^{-11} m^2 s^{-1}). In comparison, the D value of ligand **1a** in the same solvent is significantly larger because the molecular size is much smaller (D = 1.0 × 10^{-10} m^2 s^{-1}). In the structure of complex **3a** with the composition of $M_{12}(\mathbf{1a})_m(\mathbf{1b})_{24-m}$, the average of m is 18 according to the used stoichiometry, and the number of m should have a static distribution due to the random mixing of the ligands with exactly the same shape.[10i] Toward the detailed structural determination, we earnestly tried to obtain mass spectra of the product, but the trials were unsuccessful presumably due to the huge structures with high molecular weights. Using a similar procedure, $M_{12}L_{24}$ spherical complexes **3b** and **3c** composed of ligands **1a** and **1c** and **1a** and **1d**, respectively, both in a 3:1 molar ratio were synthesized.

In order to demonstrate that the dual-functionalized spheres maintain their previously observed irreversible titania-binding ability even after 25% of the minTBP-1 peptide aptamers on its surface have been replaced with biotin, QCM analyses[19] using a Ti-coated sensor were performed. When a diluted aqueous solution of **3a** (10 μM, H_2O/DMSO = 95:5 (v/v)) buffered with 9.5 mM HEPES (pH 7.5) was injected into the QCM cell, the resonance frequency (f) of the Ti-coated sensor immediately decreased, an observation that indicates that **3a** has bound to the Ti surface (Figure 3, red line). The fact that

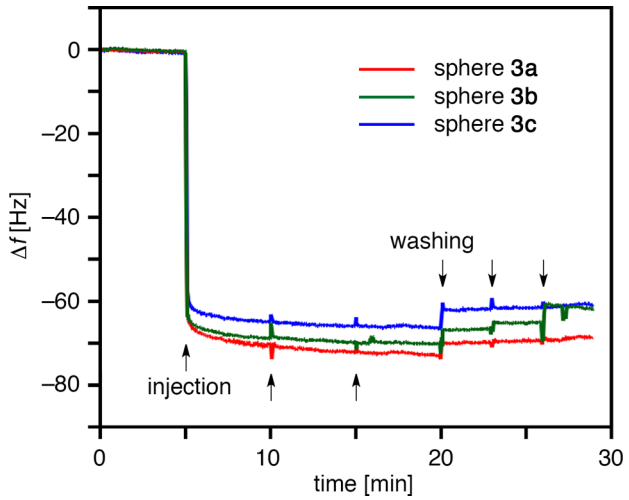

Figure 3. Changes in resonance frequency (f) as a function of time in QCM measurements. Binding and dissociation profiles for sphere **3a** (red line), **3b** (green), and **3c** (blue line) (10 μM of sphere, H_2O/DMSO = 95:5 (v/v), 9.5 mM HEPES, pH = 7.5, room temperature).

the spheres are strongly bound was confirmed by repeated washings with a buffer solution, after which the f value remained constant, proving the irreversible binding of **3a** on titania. Using Sauerbrey's equation,[19a] the mass gain on the Ti sensor was estimated to be 3.7 × 10^2 ng cm^{-2} from Δf (−70 Hz). This mass gain suggests that the sphere **3a** is densely glued on the Ti substrate in a monolayer fashion by virtue of the peptide aptamers. These results demonstrate that the original titania-binding ability of sphere **2a** (Δf = −63 Hz) is maintained. The spheres **3b** and **3c** also exhibit tight titania-binding behavior with values of Δf = −67 and −62 Hz, respectively (Figure 3, green and blue lines). Because the

DOI: 10.1021/jacs.5b06184
J. Am. Chem. Soc. 2015, 137, 12890−12896

spheres **3a**–**c** still showed irreversible fixation on titania despite the decreased surface density of the minTBP-1 aptamers by 25%, we next set out to show the fixation of streptavidin on titania via bridging adhesion made possible by these dual-functionalized spheres.

The adhesion of streptavidin on a titania surface mediated by the dual-functionalized sphere was examined by QCM analysis. The sensor chip fixing the sphere **3a** was pretreated with a solution of 50 μg/mL bovine serum albumin (BSA), a standard blocking agent to avoid nonspecific adsorption,[20] followed by the injection of an aqueous solution of streptavidin (10 μg/mL, H_2O/DMSO = 95:5 (v/v)) buffered with 9.5 mM HEPES (pH 7.5). The resonance frequency (f) of the sensor incrementally decreased as the number of repeated injections increased, an observation that indicates streptavidin was bound to the titania surface via the interaction with the biotin of sphere **3a** (Figure 4, red line). The proteins were strongly bound, as even after

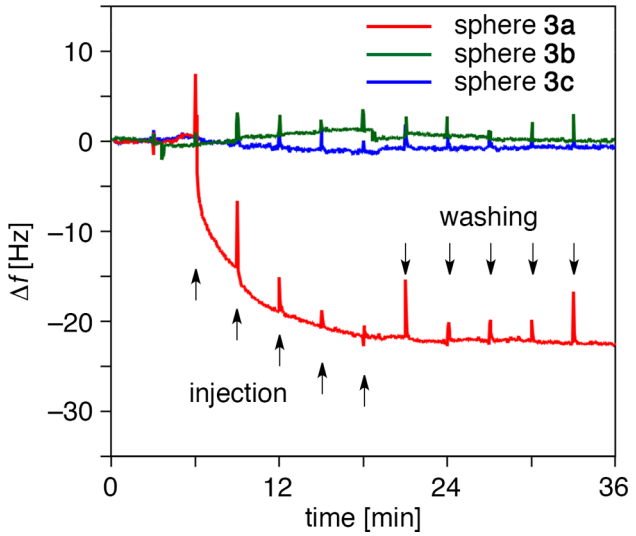

Figure 4. Changes in resonance frequency (f) as a function of time in QCM measurements. Binding and dissociation profiles for streptavidin fixed on sphere **3a** (red line), **3b** (green), and **3c** (blue line) (10 μg of streptavidin, H_2O/DMSO = 95:5 (v/v), 9.5 mM HEPES, pH = 7.5, room temperature).

repeated washings with a buffer solution the f value remained constant. When sphere **3b** composed of biotinylated ligands tethered by the shorter linker was employed, streptavidin was not observed to be fixed by the biotin–streptavidin interaction (Figure 4, green line). Because the lengths of the chains of ligands **1a**, **1b**, and **1c** are around 2.6, 4.6, and 1.6 nm, respectively, the biotins on sphere **3b** are not accessible by streptavidin, presumably due to the steric repulsion maintained by the minTBP-1 peptide chains, whereas the biotins on sphere **3a** are well exposed and accessible. As a control experiment, when sphere **3c** without biotin was employed, the fixation of streptavidin was also not observed (Figure 4, blue line).

To visualize the substrate-specific fixation of streptavidin, we used a Ti/Au micropatterned surface.[21] The patterning experiments were performed on a plate of Au with dimensions of 4 × 4 mm^2 covered with Ti using lithographic techniques (Figure 5a). The plate was dipped into the solution of **3a** (10 μM, H_2O/DMSO = 95:5 (v/v)) buffered with 10 mM HEPES (pH 7.5), 50 mM $NaNO_3$, and 0.05% Tween 20 as a blocking agent to avoid nonspecific adsorption. After the plate was

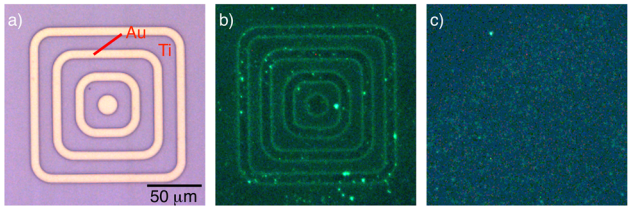

Figure 5. (a) Optical microscopic image of Ti/Au-patterned surface. (b,c) Fluorescence microscopic images of a Ti/Au-patterned surface after the addition of streptavidin on the surface (b) with sphere **3a** and (c) without sphere **3a**.

washed with an aqueous buffer, it was dipped into the solution of fluorochrome-labeled streptavidin (10 μg/mL in H_2O) buffered with 10 mM HEPES (pH 7.5), 50 mM $NaNO_3$, and 0.05% Tween 20.[20a,b] The green fluorescence image was observed for the Ti-patterned area, showing the selective fixation of the protein on the titania surface by bridging adhesion of sphere **3a** (Figure 5b). As a control experiment, when the plate was treated with the fluorochrome-labeled streptavidin without sphere **3a**, we did not observe any contrast in the fluorescence of the microscopic images (Figure 5c).

In conclusion, we have synthesized a dual-functionalized $M_{12}L_{24}$ sphere bearing both titania-specific peptide aptamers and protein recognition sites and confirmed that the sphere demonstrates bridging adhesion that brings together protein with titania surfaces in an irreversible fashion. Three-fourths of the functional groups on the periphery of the spheres were dedicated to the titania-binding peptide aptamers, and the remaining one-quarter were designated for biotin, enabling streptavidin recognition. The accumulated peptide aptamers work in a cooperative fashion to irreversibly fix the spheres on titania, while the rationally designed linker was made long enough to promote the exposure of biotin and was shown to be essential for capturing streptavidin efficiently. This present method that combines two independent modes of recognition derived from two different functional groups is a flexible and easily modifiable design strategy that enables the interdisciplinary combination of molecular biology with inorganic surface chemistry.

MATERIALS AND METHODS

General Procedure. NMR spectra were recorded on a Bruker DRX-500 equipped with 5 mm BBO probe with a z-field gradient coil or on a Bruker AV-500 equipped with a TCI CryoProbe with a z-field gradient coil. For ^{1}H and ^{13}C NMR spectra of the ligands, the D_2O solution of the ligand was placed in the sample tube together with a coaxial thin tube filled with tetramethylsilane (TMS) in $CDCl_3$ solution, and the spectra were referenced internally to TMS as a standard. For the spheres, ^{1}H NMR spectra were referenced internally to a solvent resonance as a standard. Methyl, methylene, and methyne signals of ^{13}C NMR were assigned by DEPT experiments. IR measurements were carried out as KBr pellets using a DIGILAB FTS-7000 instrument. MALDI TOF MS (matrix-assisted laser desorption ionization time-of-flight mass spectrometry) was performed on an Applied Biosystems BioSpectrometry Workstation model Voyager-DE STR spectrometer. Elemental analyses for carbon, hydrogen, and nitrogen were performed on a Yanaco MT-6. Melting points were determined on a Yanaco MP-500 V melting-point apparatus. QCM measurements were performed on a Q-Sense AB QCM-D300 instrument using a Ti sputter-coated QCM sensor. UV/ozone surface treatment for the QCM sensor was performed on a BioForceNanosciences Inc. ProCleaner. Optical and fluorescence microscopic images

DOI: 10.1021/jacs.5b06184
J. Am. Chem. Soc. 2015, 137, 12890–12896

were taken with Leica DMLP equipped with a mercury lamp and a 480/527 filter set (LS, Leica).

Solvents and reagents were purchased from TCI Co., Ltd., and WAKO Pure Chemical Industries Ltd. Fmoc amino acids and some reagents for the peptide synthesis were purchased from Watanabe Chemical Industries Ltd. Streptavidin, fluorochrome-labeled streptavidin (Alexa Fluor 488 streptavidin conjugate), and BSA were purchased from Sigma-Aldrich Japan Co. LLC, Invitrogen Co. Ltd., and Iwai Chemicals Co., Ltd., respectively. All chemicals were used without any further purification. Automated peptide synthesis was performed on an Applied Biosystems ABI 433A. Peptides were purified on a reversed-phase HPLC (high-performance liquid chromatography) system equipped with a Develosil ODS preparative column (ODS-15/30 (50 × 500 mm), Nomura Chemical). Ligands **1a**,**d**,**e** were synthesized according to the reported procedures.[10a,16]

Syntheses of Ligands. *Ligand **1b***. Protected peptide, biotin-$(Ala)_5$-Lys(Boc)-Leu-Pro-Asp(O*t*-Bu)-Ala-OH, synthesized from H-Ala-2-Cl-Trt-resin (0.25 mmol), HBTU (114 mg, 0.300 mmol), HOBt (41 mg, 0.30 mmol), and DIPEA (174 mL, 1.00 mmol) were dissolved in 10 mL of DMF under an argon atmosphere, and 2-(3,5-di(pyridin-4-yl)phenoxy)ethylamine (87 mg, 0.30 mmol) was added to the solution. The reaction mixture was stirred overnight at room temperature. The solvent was removed in vacuo, and the deprotection reaction for the crude mixture was performed by adding water (0.5 mL) and trifluoroacetic acid (9.5 mL) followed by stirring of the solution for 2 h at room temperature. Volatile chemicals were removed in vacuo, and a crude mixture was obtained by adding an excess amount of ether. Ligand **1b** was obtained as a white powder after HPLC purification in 42% yield (185 mg, 0.106 mmol) from the starting resin: mp 171−174 °C; IR (KBr, cm^{-1}) 3422, 3069, 2938, 1670, 1534, 1522, 1454, 1201, 1134, 1048, 829, 722; MALDI TOF MS *m*/*z* calcd for $[M + H]^+$ 1397.7, found 1397.7; ^1H NMR (500 MHz, 300 K, D_2O) δ 8.83 (d, J = 5.9 Hz, 4H), 8.32 (d, J = 5.9 Hz, 4H), 7.94 (s, 1H), 7.66 (s, 2H), 4.63−4.55 (m, 2H), 4.46 (t, J = 6.7 Hz, 1H), 4.42 (t, J = 5.8 Hz, 1H), 4.36−4.22 (m, 10H), 3.84−3.54 (m, 4H), 3.36−3.29 (m, 1H), 3.03−2.96 (m, 3H), 2.77 (d, J = 13 Hz, 1H), 2.70−2.53 (m, 2H), 2.31 (t, J = 7.0 Hz, 2H), 2.27−2.16 (m, 1H), 2.03−1.93 (m, 2H), 1.88−1.78 (m, 2H), 1.78−1.50 (m, 7H), 1.39 (t, J = 7.9 Hz, 24H), 0.91 (d, J = 6.5 Hz, 3H), 0.88 (d, J = 6.3 Hz, 3H); ^{13}C NMR (125 MHz, 300 K, D_2O) δ 177.08 (C), 176.20 (C), 175.60 (C), 175.22 (C), 175.12 (C), 175.04 (C), 174.86 (C), 174.83 (C), 174.07 (C), 173.59 (C), 172.82 (C), 172.26 (C), 165.44 (C), 159.60 (C), 155.89 (C), 142.40 (CH), 137.86 (C), 124.71 (CH), 120.36 (CH), 117.08 (CH), 67.14 (CH_2), 62.13 (CH), 60.65 (CH), 60.33 (CH), 55.44 (CH), 53.15 (CH), 51.24 (CH), 50.43 (CH), 50.22 (CH), 50.00 (CH), 49.86 (2CH), 49.75 (CH), 49.69 (CH), 47.85 (CH_2), 39.78 (CH_2), 39.26 (CH_2), 38.90 (CH_2), 37.32 (CH_2), 34.93 (CH_2), 30.36 (CH_2), 29.29 (CH_2), 27.97 (CH_2), 27.78 (CH_2), 26.26 (CH_2), 25.01 (CH_2), 24.73 (CH_2), 24.43 (CH), 22.48 (CH_3), 22.04 (CH_2), 20.51 (CH_3), 16.60 (CH_3), 16.51 (CH_3), 16.42 (CH_3), 16.40 ($2CH_3$), 16.30 (CH_3). Anal. Calcd for $C_{67}H_{96}N_{16}O_{15}S{\cdot}3TFA{\cdot}5.5H_2O$: C, 47.68; H, 6.03; N, 12.19. Found: C, 48.08; H, 6.10; N, 11.81.

*Ligand **1c***. Biotin (24.1 mg, 0.986 mmol), HBTU (45.0 mg, 0.646 mmol), HOBt (21.0 mg, 0.155 mmol), and DIPEA (50.0 mL, 0.287 mmol) were dissolved in 10 mL of DMF under an argon atmosphere, and 2-(3,5-di(pyridin-4-yl)phenoxy)ethylamine (87 mg, 0.30 mmol) was added to the solution. The reaction mixture was stirred overnight at room temperature. The solvent was removed in vacuo. Ligand **1c** was obtained as a white powder after HPLC purification in 77% yield (57.0 mg, 0.765 mmol): mp >160 °C (decomposed); IR (KBr, cm^{-1}) 3427, 3084, 2937, 1686, 1636, 1596, 1512, 1430, 1348, 1202, 1133, 821, 722; MALDI TOF MS *m*/*z* calcd for $[M + H]^+$ 518.1, found 518.2; ^1H NMR (500 MHz, 300 K, D_2O) δ 8.81 (d, J = 6.6 Hz, 4H), 8.28 (d, J = 6.6 Hz, 4H), 7.93 (s, 1H), 7.65 (s, 2H), 4.35−4.35 (m, 3H), 4.06−4.02 (m, 1H), 3.73−3.63 (m, 2H), 2.64 (d, J = 4.8 Hz, 1H), 2.62 (d, J = 4.8 Hz, 1H), 2.42 (d, J = 13.2 Hz, 1H), 2.32−2.20 (m, 2H), 1.67−1.45 (m, 3H), 1.24−1.15 (m, 3H); ^{13}C NMR (125 MHz, 300 K, D_2O) δ 177.17 (C), 164.96 (C), 155.36 (C), 142.73 (CH), 137.92 (C), 124.49 (CH), 120.15 (CH), 116.84 (CH), 67.69 (CH_2), 61.76 (CH), 60.08 (CH), 55.19 (CH), 39.65 (CH_2), 38.92 (CH_2), 35.65 (CH_2), 27.69 (CH_2), 27.50 (CH_2), 25.22 (CH_2).

Syntheses of Spheres. *Sphere **3a***. Ligand **1a** (11.1 mg, 7.50 μmol), ligand **1b** (4.35 mg, 2.50 μmol), and $Pd(NO_3)_2$ (1.61 mg, 7.00 μmol) were dissolved in 1.00 mL of DMSO. The reaction mixture was stirred for 24 h at 70 °C, affording sphere **3a** as a brown solution: mp >240 °C (decomposed); IR (KBr, cm^{-1}) 3410, 3075, 2955, 1659, 1643, 1530, 1410, 1383, 1349, 1200, 1136, 954, 834; ^1H NMR (500 MHz, 300 K, DMSO-d_6) δ 9.50 (br, 96H), 8.40 (br, 96H), 8.17 (br, NH), 8.08 (br, 24H + NH), 7.94 (br, NH), 7.74 (br, NH), 7.68 (br, NH), 7.58 (br, 48H), 4.48 (br, 36H), 4.22 (br, 144H), 3.62 (br, 24H), 3.49 (br, 60H), 3.08 (br, 36H), 2.74 (br, 48H), 2.18 (br, 6H), 2.12 (br, 12H), 2.03 (br, 24H), 1.91 (br, 24H), 1.85 (s, 54H), 1.80 (br, 48H), 1.63 (br, 72H), 1.48 (br, 180H), 1.28 (br, 72H), 1.19 (br, 162H), 0.85 (br, 144H). Anal. Calcd for $C_{1302}H_{1854}N_{354}O_{342}S_6Pd_{12}{\cdot}42TFA{\cdot}120H_2O$: C, 45.79; H, 5.92; N, 13.64. Found: C, 45.89; H, 5.99; N, 13.83.

*Sphere **3b***. Ligand **1a** (3.30 mg, 2.25 μmol), ligand **1c** (0.56 mg, 0.75 μmol), and $Pd(NO_3)_2$ (0.48 mg, 2.1 μmol) were dissolved in 0.60 mL of DMSO. The reaction mixture was stirred for 24 h at 70 °C, affording sphere **3a** as a brown solution: ^1H NMR (500 MHz, 300 K, DMSO-d_6) δ 9.52 (br, 96H), 8.40 (br, 96H), 8.12 (br, NH), 8.07 (br, 24H), 7.95 (br, NH), 7.72 (br, NH), 7.66 (br, NH), 7.58 (br, 48H), 4.49 (br, 18H), 4.24 (br, 36H), 3.63 (br, 36H), 3.50 (br, 36H), 3.08 (br, 36H), 2.75 (br, 72H), 2.02 (br, 18H), 1.85 (s, 54H), 1.90 (br, 18H), 1.81 (br, 36H), 1.64 (br, 54H), 1.48 (br, 144H), 1.35−1.10 (br, 90H), 0.86 (br, 108H).

*Sphere **3c***. Ligand **1a** (14.8 mg, 10.0 μmol), ligand **1d** (0.77 mg, 3.3 μmol), and $Pd(NO_3)_2$ (2.15 mg, 9.33 μmol) were dissolved in 1.33 mL of DMSO. The reaction mixture was stirred for 24 h at 70 °C, affording sphere **3a** as a brown solution: mp >230 °C (decomposed); IR (KBr, cm^{-1}) 3352, 3080, 2956, 1654, 1617, 1541, 1383, 1201, 1136, 1024, 954, 829; ^1H NMR (500 MHz, 300 K, DMSO-d_6) δ 9.51 (br, 96H), 8.39 (br, 96H), 8.21 (br, NH), 8.17 (br, NH), 8.07 (br, 24H + NH), 7.95 (br, NH), 7.73 (br, NH), 7.68 (br, NH), 7.56 (br, 48H), 4.70−4.50 (br, 144H), 3.62 (br, 36H), 3.50 (br, 36H), 3.08 (br, 36H), 2.75 (br, 72H), 2.02 (br, 18H), 1.90 (br, 18H), 1.85 (s, 54H), 1.82 (br, 36H), 1.63 (br, 54H), 1.48 (br, 144H), 1.28 (br, 36H), 1.23−1.14 (br, 54H), 0.86 (br, 108H). Anal. Calcd for $C_{996}H_{1350}N_{270}O_{252}Pd_{12}{\cdot}36TFA{\cdot}144H_2O$: C, 44.06; H, 5.80; N, 12.99. Found: C, 44.23; H, 6.08; N, 13.28.

QCM Analyses. Prior to measurements, the sensor was cleaned for 10 min using a UV/ozone surface treatment system. The measurements were carried out at 25 °C, and the analytical data were collected at 14.8 MHz. The sensor was first equilibrated with 100 mM HEPES (pH 7.5) buffer and an aqueous solution (H_2O/DMSO = 95:5 (v/v)) buffered with 9.5 mM HEPES (pH 7.5), successively, followed by the injection of a 10 μM aqueous solution of sphere **3** (H_2O/DMSO = 95:5 (v/v)) buffered with 9.5 mM HEPES (pH 7.5). The sensor surface was washed with an aqueous solution (H_2O/DMSO = 95:5 (v/v)) buffered with 9.5 mM HEPES (pH 7.5) and 10 mM HEPES (pH 7.5) buffer, successively, and treated with 50 μg/mL BSA buffered with 10 mM HEPES (pH 7.5), followed by washing with 10 mM HEPES (pH 7.5) buffer. Then, an aqueous solution of 10 μg/mL streptavidin buffered with 10 mM HEPES (pH 7.5) was injected, followed by washing with 10 mM HEPES (pH 7.5) buffer.

Patterning Experiments. Prior to measurements, the plate with the lithographic pattern was cleaned for 10 min using a UV/ozone surface treatment system. The plate was first equilibrated with 100 mM HEPES (pH 7.5) buffer (200 μL) for 1 h and an aqueous solution (200 μL, H_2O/DMSO = 95:5 (v/v)) buffered with 9.5 mM HEPES (pH 7.5), 50 mM $NaNO_3$, and 0.05% Tween 20 for 1.5 h, successively, followed by the treatment with an aqueous 10 μM solution of sphere **3** (200 μL, H_2O/DMSO = 95:5 (v/v)) buffered with 9.5 mM HEPES (pH 7.5), 50 mM $NaNO_3$, and 0.05% Tween 20 for 1 min. The plate was washed three times with an aqueous solution (200 μL, H_2O/DMSO = 95:5 (v/v)) buffered with 9.5 mM HEPES (pH 7.5), 50 mM $NaNO_3$, and 0.05% Tween 20 for 10 min and three times with 10 mM HEPES (pH 7.5), 50 mM $NaNO_3$, and 0.05% Tween 20 buffer (200 μL) for 10 min. Then, the sensor was treated with an aqueous solution

DOI: 10.1021/jacs.5b06184
J. Am. Chem. Soc. 2015, 137, 12890−12896

of 10 μg/mL fluorochrome-labeled streptavidin buffered with 10 mM HEPES (pH 7.5), 50 mM $NaNO_3$, and 0.05% Tween 20 buffer (200 μL), followed by washing three times with 10 mM HEPES (pH 7.5), 50 mM $NaNO_3$, and 0.05% Tween 20 buffer (200 μL) for 10 min and three times with 10 mM HEPES (pH 7.5) buffer (200 μL) for 10 min. The microscopic images of the resultant plate were performed with a cover glass on the plate at room temperature.

■ ASSOCIATED CONTENT

Supporting Information

NMR spectra of ligands and spheres. The Supporting Information is available free of charge on the ACS Publications website at DOI: 10.1021/jacs.5b06184.

■ AUTHOR INFORMATION

Corresponding Authors

*satosota@m.tohoku.ac.jp
*kshiba@jfcr.or.jp
*mfujita@appchem.t.u-tokyo.ac.jp

Notes

The authors declare no competing financial interest.

■ ACKNOWLEDGMENTS

We thank Ms. Tamiko Minamisawa for her help with the QCM measurements. This research was supported by JST, ACCEL to M.F., MEXT KAKENHI (25102007, 24685010, 23107509) to S.S., and JST, CREST, to K.S.

■ REFERENCES

(1) (a) Lequin, R. M. *Clin. Chem.* **2005**, *51*, 2415−2418. (b) Van Weemen, B. K.; Schuurs, A. H. W. M. *FEBS Lett.* **1971**, *15*, 232−236.

(2) (a) Cheung, V. G.; Morley, M.; Aguilar, F.; Massimi, A.; Kucherlapati, R.; Childs, G. *Nat. Genet.* **1999**, *21*, 15−19. (b) Debouck, C.; Goodfellow, P. N. *Nat. Genet.* **1999**, *21*, 48−50. (c) Sassolas, A.; Leca-Bouvier, B. D.; Blum, L. J. *Chem. Rev.* **2008**, *108*, 109−139.

(3) (a) Jonkheijm, P.; Weinrich, D.; Schroder, H.; Niemeyer, C. M.; Waldmann, H. *Angew. Chem., Int. Ed.* **2008**, *47*, 9618−9647. (b) Weinrich, D.; Jonkheijm, P.; Niemeyer, C. M.; Waldmann, H. *Angew. Chem., Int. Ed.* **2009**, *48*, 7744−7751. (c) Wong, L. S.; Khan, F.; Micklefield, J. *Chem. Rev.* **2009**, *109*, 4025−4053.

(4) (a) Dickerson, M. B.; Sandhage, K. H.; Naik, R. R. *Chem. Rev.* **2008**, *108*, 4935−4978. (b) Nudelman, F.; Sommerdijk, N. A. J. M. *Angew. Chem., Int. Ed.* **2012**, *51*, 6582−6596.

(5) Joddar, B.; Ito, Y. *J. Mater. Chem.* **2011**, *21*, 13737−13755.

(6) (a) Brunette, D.; Tengvall, P.; Textor, M.; Thomsen, P. *Titanium in Medicine*; Springer-Verlag: Berlin, 2001. (b) Schuler, M.; Trentin, D.; Textor, M.; Tosatti, S. G. *Nanomedicine* **2006**, *1*, 449−463. (c) Le Guehennec, L.; Soueidan, A.; Layrolle, P.; Amouriq, Y. *Dent. Mater.* **2007**, *23*, 844−854. (d) de Jonge, L. T.; Leeuwenburgh, S. C. G.; Wolke, J. G. C.; Jansen, J. A. *Pharm. Res.* **2008**, *25*, 2357−2369.

(7) (a) Kokubun, K.; Kashiwagi, K.; Yoshinari, M.; Inoue, T.; Shiba, K. *Biomacromolecules* **2008**, *9*, 3098−3105. (b) Kashiwagi, K.; Tsuji, T.; Shiba, K. *Biomaterials* **2009**, *30*, 1166−1175.

(8) (a) Kriplani, U.; Kay, B. K. *Curr. Opin. Biotechnol.* **2005**, *16*, 470−475. (b) Baneyx, F.; Schwartz, D. T. *Curr. Opin. Biotechnol.* **2007**, *18*, 312−317. (c) Mascini, M.; Palchetti, I.; Tombelli, S. *Angew. Chem., Int. Ed.* **2012**, *51*, 1316−1332.

(9) (a) Tominaga, M.; Suzuki, K.; Murase, T.; Fujita, M. *J. Am. Chem. Soc.* **2005**, *127*, 11950−11951. (b) Murase, T.; Sato, S.; Fujita, M. *Angew. Chem., Int. Ed.* **2007**, *46*, 1083−1085. (c) Suzuki, K.; Kawano, M.; Sato, S.; Fujita, M. *J. Am. Chem. Soc.* **2007**, *129*, 10652−10653. (d) Murase, T.; Sato, S.; Fujita, M. *Angew. Chem., Int. Ed.* **2007**, *46*, 5133−5136. (e) Sun, Q.-F.; Sato, S.; Fujita, M. *Chem. Lett.* **2011**, *40*, 726−727. (f) Sato, S.; Murase, T.; Fujita, M. Self-Assembly of Coordination Cages and Spheres. In *Supramolecular Chemistry: From Molecules to Nanomaterials*; Steed, J. W., Gale, P. A., Eds.; John Wiley & Sons: Chichester, U.K., 2012; Vol. *5*, pp 2071−2084.

(10) (a) Tominaga, M.; Suzuki, K.; Kawano, M.; Kusukawa, T.; Ozeki, T.; Sakamoto, S.; Yamaguchi, K.; Fujita, M. *Angew. Chem., Int. Ed.* **2004**, *43*, 5621−5625. (b) Suzuki, K.; Kawano, M.; Fujita, M. *Angew. Chem., Int. Ed.* **2007**, *46*, 2819−2822. (c) Suzuki, K.; Tominaga, M.; Kawano, M.; Fujita, M. *Chem. Commun.* **2009**, 1638−1640. (d) Sun, Q.-F.; Iwasa, J.; Ogawa, D.; Ishido, Y.; Sato, S.; Ozeki, T.; Sei, Y.; Yamaguchi, K.; Fujita, M. *Science* **2010**, *328*, 1144−1147. (e) Fujita, D.; Takahashi, A.; Sato, S.; Fujita, M. *J. Am. Chem. Soc.* **2011**, *133*, 13317−13319. (f) Sun, Q.-F.; Murase, T.; Sato, S.; Fujita, M. *Angew. Chem., Int. Ed.* **2011**, *50*, 10318−10321. (g) Bunzen, J.; Iwasa, J.; Bonakdarzadeh, P.; Numata, E.; Rissanen, K.; Sato, S.; Fujita, M. *Angew. Chem., Int. Ed.* **2012**, *51*, 3161−3163. (h) Sun, Q.-F.; Sato, S.; Fujita, M. *Nat. Chem.* **2012**, *4*, 330−333. (i) Sun, Q.-F.; Sato, S.; Fujita, M. *Angew. Chem., Int. Ed.* **2014**, *53*, 13510−13513. (j) Fujita, D.; Yokoyama, H.; Ueda, Y.; Sato, S.; Fujita, M. *Angew. Chem., Int. Ed.* **2015**, *54*, 155−158.

(11) (a) Sato, S.; Iida, J.; Suzuki, K.; Kawano, M.; Ozeki, T.; Fujita, M. *Science* **2006**, *313*, 1273−1276. (b) Kikuchi, T.; Murase, T.; Sato, S.; Fujita, M. *Supramol. Chem.* **2008**, *20*, 81−94. (c) Suzuki, K.; Iida, J.; Sato, S.; Kawano, M.; Fujita, M. *Angew. Chem., Int. Ed.* **2008**, *47*, 5780−5782. (d) Suzuki, K.; Takao, K.; Sato, S.; Fujita, M. *J. Am. Chem. Soc.* **2010**, *132*, 2544−2545. (e) Bruns, C. J.; Fujita, D.; Hoshino, M.; Sato, S.; Stoddart, J. F.; Fujita, M. *J. Am. Chem. Soc.* **2014**, *136*, 12027−12034.

(12) (a) Kamiya, N.; Tominaga, M.; Sato, S.; Fujita, M. *J. Am. Chem. Soc.* **2007**, *129*, 3816−3817. (b) Kikuchi, T.; Sato, S.; Fujita, M. *J. Am. Chem. Soc.* **2010**, *132*, 15930−15932. (c) Fujita, D.; Suzuki, K.; Sato, S.; Yagi-Utsumi, M.; Kurimoto, E.; Kato, K.; Fujita, M. *Chem. Lett.* **2012**, *41*, 313−315. (d) Fujita, D.; Suzuki, K.; Sato, S.; Yagi-Utsumi, M.; Yamaguchi, Y.; Mizuno, N.; Kumasaka, T.; Takata, M.; Noda, M.; Uchiyama, S.; Kato, K.; Fujita, M. *Nat. Commun.* **2012**, *3*, 1093. (e) Kikuchi, T.; Sato, S.; Fujita, D.; Fujita, M. *Chem. Sci.* **2014**, *5*, 3257−3260.

(13) (a) Suzuki, K.; Sato, S.; Fujita, M. *Nat. Chem.* **2010**, *2*, 25−29. (b) Suzuki, K.; Takao, K.; Sato, S.; Fujita, M. *Angew. Chem., Int. Ed.* **2011**, *50*, 4858−4861. (c) Takao, K.; Suzuki, K.; Ichijo, T.; Sato, S.; Asakura, H.; Teramura, K.; Kato, K.; Ohba, T.; Morita, T.; Fujita, M. *Angew. Chem., Int. Ed.* **2012**, *51*, 5893−5896. (d) Ichijo, T.; Sato, S.; Fujita, M. *J. Am. Chem. Soc.* **2013**, *135*, 6786−6789.

(14) (a) Sano, K.; Shiba, K. *J. Am. Chem. Soc.* **2003**, *125*, 14234−14235. (b) Sano, K.; Sasaki, H.; Shiba, K. *Langmuir* **2005**, *21*, 3090−3095. (c) Hayashi, T.; Sano, K.; Shiba, K.; Kumashiro, Y.; Iwahori, K.; Yamashita, I.; Hara, M. *Nano Lett.* **2006**, *6*, 515−519.

(15) (a) Sano, K.; Ajima, K.; Iwahori, K.; Yudasaka, M.; Iijima, S.; Yamashita, I.; Shiba, K. *Small* **2005**, *1*, 826−832. (b) Yamashita, I.; Kirimura, H.; Okuda, M.; Nishio, K.; Sano, K.; Shiba, K.; Hayashi, T.; Hara, M.; Mishima, Y. *Small* **2006**, *2*, 1148−1152. (c) Matsukawa, N.; Nishio, K.; Sano, K.; Shiba, K.; Yamashita, I. *Langmuir* **2009**, *25*, 3327−3330.

(16) Ikemi, M.; Kikuchi, T.; Matsumura, S.; Shiba, K.; Sato, S.; Fujita, M. *Chem. Sci.* **2010**, *1*, 68−71.

(17) (a) Wilchek, M.; Bayer, E. A. *Anal. Biochem.* **1988**, *171*, 1−32. (b) Weber, P. C.; Ohlendorf, D. H.; Wendoloski, J. J.; Salemme, F. R. *Science* **1989**, *243*, 85−88.

(18) (a) Sato, S.; Ishido, Y.; Fujita, M. *J. Am. Chem. Soc.* **2009**, *131*, 6064−6065. (b) Yoneya, M.; Tsuzuki, S.; Yamaguchi, T.; Sato, S.; Fujita, M. *ACS Nano* **2014**, *8*, 1290−1296.

(19) (a) Sauerbrey, G. *Eur. Phys. J. A* **1959**, *155*, 206−222. (b) O'Sullivan, C. K.; Guilbault, G. G. *Biosens. Bioelectron.* **1999**, *14*, 663−670. (c) Marx, K. A. *Biomacromolecules* **2003**, *4*, 1099−1120.

(20) (a) Kenna, J. G.; Major, G. N.; Williams, R. S. *J. Immunol. Methods* **1985**, *85*, 409−419. (b) Wedege, E.; Svenneby, G. *J. Immunol. Methods* **1986**, *88*, 233−237. (c) Vogt, R. F.; Phillips, D. L.; Henderson, L. O.; Whitfield, W.; Spierto, F. W. *J. Immunol. Methods* **1987**, *101*, 43−50.

(21) (a) Blawas, A. S.; Reichert, W. M. *Biomaterials* **1998**, *19*, 595−609. (b) MacBeath, G.; Schreiber, S. L. *Science* **2000**, *289*, 1760−1763.

DOI: 10.1021/jacs.5b06184
J. Am. Chem. Soc. 2015, 137, 12890−12896

(c) Ekblad, T.; Liedberg, B. *Curr. Opin. Colloid Interface Sci.* **2010**, *15*, 499−509.

DOI: 10.1021/jacs.5b06184
J. Am. Chem. Soc. 2015, 137, 12890−12896